Polarized vector oscillons

Hong-Yi Zhang, Mudit Jain, and Mustafa A. Amin

Phys. Rev. D **105**, 096037 — Published 27 May 2022

DOI: 10.1103/PhysRevD.105.096037

Polarized Vector Oscillons

Hong-Yi Zhang,* Mudit Jain,† and Mustafa A. Amin‡
Department of Physics and Astronomy, Rice University, Houston, TX 77005, USA

Oscillons are spatially localized, time-periodic and long-lived configurations that were primarily proposed in scalar field theories with attractive self-interactions. In this letter, we demonstrate that oscillons also exist in the low-energy effective theory of an interacting massive (real) vector field. We provide two types of vector oscillons with vanishing orbital angular momentum, and approximately spherically symmetric energy density, but not field configurations. These are: (1) "directional" oscillons (linearly polarized), with vanishing total intrinsic spin, and (2) "spinning" oscillons (circularly polarized) with a macroscopic instrinsic spin equal to $\hbar\times$ number of particles in the oscillon. In contrast to the case with only gravitational interactions, the two oscillons have different energy at a fixed particle number even in the nonrelativistic limit. By carrying out relativistic $3+1$d simulations, we show that these oscillons can be long-lived (compared to the oscillation time for the fields), and can arise from a range of Gaussian initial spatial profiles. These considerations make vector oscillons potentially relevant during the early universe and in dark photon dark matter, with novel phenomenology related to their polarization.

Introduction.– Non-topological solitons arise due to a balance between attractive self-interaction and dispersion in field theories. They have been realized in a broad variety of contexts in nature, from water waves [1] to Bose-Einstein condensates (BEC) [2–5]. They might also play a role in astrophysics and cosmology, with novel signatures in phase transitions in the early universe [6–10], in the formation of structure and gravitational clustering [11–17], production of gravitational waves [18–26] and electromagnetic radiation [27–30], formation of black holes [31–35], and even play a role in baryogenesis [36, 37]. While massive scalar fields and their solitons have been explored extensively in the literature (for reviews, see [38–40]), Nature provides us with many examples of higher spin fields. For instance, W and Z bosons in the Standard Model of particle physics, or speculatively, as (some or all of) dark matter [41–49].

In this letter we study non-topological solitons in real-valued massive vector fields with attractive self-interactions. These spatially localized solitons are "maximally" polarized (with respect to a particular direction), i.e. either the vector field configuration is primarily linearly polarized which we call a "directional" oscillon, or it is mostly circularly polarized that we refer to as a "spinning" oscillon (see Fig. 1 for a quick description). Such objects might be present in the post-inflationary universe or constitute part of the present-day dark matter, and can provide novel gravitational and non-gravitational signatures revealing the intrinsic spin of the underlying massive (dark) vector field.

Although vector solitons can be supported solely by gravitational interactions [50, 51], self-interactions may appear naturally in the low-energy limit of an interacting vector field theory and play an important role in their phenomenology. For example, in the early universe, they can have a dominant effect in early structure formation [9, 52–54]. As we will show, self-interactions can also explicitly lift the degeneracy in energy between the directional and spinning oscillons, potentially determining which type of oscillon can form more easily. Furthermore, matter-wave solitons in BECs [2–5] and electromagnetic solitons in nonlinear media (optical fibres) [55–59] owe their existence to attractive self-interactions.

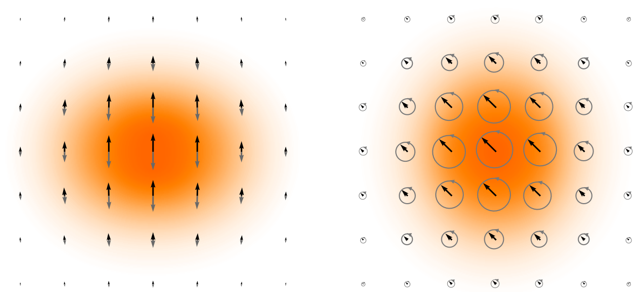

FIG. 1. The directional and spinning oscillons obtained from relativistic simulations. The energy densities are approximately spherically symmetric, but the field configurations are not. For the spinning oscillon (right), the vector field at each point moves in a circle, resulting in a macroscopic intrinsic spin. For the directional oscillon (left), the field oscillates along an approximately fixed direction and has zero spin.

In what follows, we begin by studying vector oscillons using nonrelativistic approximations, and then perform fully relativistic numerical simulations to confirm their stability, longevity, etc. Finally, we summarize our results and discuss potential implications. Additional details and results are provided in the Supplemental Material. We work in natural units and adopt mostly plus signature for the metric.

Model.– We study a real-valued massive spin-1 field W_μ with the Lagrangian

$$\mathcal{L} = -\frac{1}{4}X_{\mu\nu}X^{\mu\nu} - V(W_\mu W^\mu)\,, \qquad (1)$$

where $X_{\mu\nu} = \partial_\mu W_\nu - \partial_\nu W_\mu$ and the potential

$$V(W_\mu W^\mu) = \frac{m^2}{2} W_\mu W^\mu - \frac{\lambda}{4}(W_\mu W^\mu)^2 + \frac{\gamma}{6}(W_\mu W^\mu)^3 + \ldots \tag{2}$$

with positive couplings λ and γ. Such effective potentials, for example, could naturally arise in the low-energy regime of interacting massive vector fields [60]. The Euler-Lagrange equations are

$$\begin{aligned}&\nabla^2 W_0 - \partial_t \nabla \cdot \boldsymbol{W} - 2V'(W_\mu W^\mu) W_0 = 0, \qquad (3)\\ &\partial_t^2 \boldsymbol{W} - \partial_t \nabla W_0 + \nabla \times (\nabla \times \boldsymbol{W}) + 2V'(W_\mu W^\mu)\boldsymbol{W} = 0.\end{aligned}$$

Using the Noether energy-momentum tensor $T^{\mu\nu} = \partial^\nu W_\sigma X^{\mu\sigma} + \eta^{\mu\nu}\mathcal{L}$, the energy $E \equiv \int \mathrm{d}^3x\, T^{00}$ is given by

$$E = \int \mathrm{d}^3x \left[\frac{1}{2}\left(\dot{\boldsymbol{W}} - \nabla W_0\right)^2 + \frac{1}{2}\left(\nabla \times \boldsymbol{W}\right)^2 + 2W_0^2 V' + V\right], \tag{4}$$

where we have used the equations of motion and also discarded a boundary term to get the explicit expression above. Furthermore, the conserved 4-current associated with Lorentz invariance is $\mathcal{M}^{\mu\nu\sigma} = \mathcal{L}^{\mu\nu\sigma} + \mathcal{S}^{\mu\nu\sigma}$. We have separated out $\mathcal{L}^{\mu\nu\sigma} = x^\nu T^{\mu\sigma} - x^\sigma T^{\mu\nu}$ and $\mathcal{S}^{\mu\nu\sigma} = X^{\mu\nu} W^\sigma - X^{\mu\sigma} W^\nu$ so that the orbital and spin angular momentum densities are $L_i = (1/2)\epsilon_{ijk}\mathcal{L}^{0jk}$ and $S_i = (1/2)\epsilon_{ijk}\mathcal{S}^{0jk}$ respectively. In particular, the spin density is

$$\boldsymbol{S} = \boldsymbol{W} \times \left(\dot{\boldsymbol{W}} - \nabla W_0\right), \tag{5}$$

which will play a pivotal role in discriminating the directional and spinning oscillon configurations.

Nonrelativistic limit.– It turns out to be sufficient to consider the nonrelativistic regime of the theory in the sense that $|\nabla^2/m^2| \lesssim 10^{-2}$. We express the real vector field $\boldsymbol{W}$ in terms of a complex vector field $\boldsymbol{\Psi}$, i.e.

$$\boldsymbol{W}(t, \boldsymbol{x}) \equiv \sqrt{\frac{2}{m}}\,\Re\left[\boldsymbol{\Psi}(t, \boldsymbol{x}) e^{-imt}\right], \tag{6}$$

and $W_0(t, \boldsymbol{x}) \equiv \sqrt{2/m}\,\Re\left[\psi_0(t, \boldsymbol{x}) e^{-imt}\right]$, where the dependence of $\boldsymbol{\Psi}$ and ψ_0 on time is assumed to be weak. Upon plugging this expansion into the action, dropping all terms with the oscillatory factors $e^{\pm inmt}$ ($n \geq 2$), and keeping only the leading-order terms in time and spatial derivatives of $\boldsymbol{\Psi}$ (see, for example [13, 50, 51, 61–63]), we get the following effective nonrelativistic Lagrangian density

$$\mathcal{L} = \Re[i\boldsymbol{\Psi}^\dagger \dot{\boldsymbol{\Psi}}] - \frac{1}{2m}\nabla\boldsymbol{\Psi}^\dagger \cdot \nabla\boldsymbol{\Psi} - V_{\rm nl}(\boldsymbol{\Psi}^\dagger, \boldsymbol{\Psi}), \tag{7}$$

where we have solved for the constraint equation (to working order in $|\nabla^2/m^2|$), $\psi_0 = i\nabla \cdot \boldsymbol{\Psi}/m$ and the non-linear potential is

$$V_{\rm nl}(\boldsymbol{\Psi}^\dagger, \boldsymbol{\Psi}) = -\frac{3\lambda}{8m^2}(\boldsymbol{\Psi}^\dagger\boldsymbol{\Psi})^2 + \frac{5\gamma}{12m^3}(\boldsymbol{\Psi}^\dagger\boldsymbol{\Psi})^3 + \left[\frac{\lambda}{8m^2} - \frac{\gamma}{4m^3}(\boldsymbol{\Psi}^\dagger\boldsymbol{\Psi})\right](\boldsymbol{S} \cdot \boldsymbol{S}). \tag{8}$$

Note that we are able to write $V_{\rm nl}$ in terms of $\boldsymbol{\Psi}^\dagger\boldsymbol{\Psi}$, and the spin density $\boldsymbol{S} = i\,\boldsymbol{\Psi} \times \boldsymbol{\Psi}^\dagger$, which is the nonrelativistic, slowly varying part of (5). This spin density can also be obtained directly from the rotational invariance of the nonrelativistic action for $\boldsymbol{\Psi}$. The appearance of $\boldsymbol{S} \cdot \boldsymbol{S}$ in $V_{\rm nl}$ suggests that the spin density will play a role in determining the energy of our solutions. This energy is given by

$$\mathcal{E} = \int \mathrm{d}^3x \left[\frac{1}{2m}\nabla\boldsymbol{\Psi}^\dagger \cdot \nabla\boldsymbol{\Psi} + V_{\rm nl}\right], \tag{9}$$

which is the sum of the kinetic and potential energy, and can be obtained from the nonrelativistic action. The total energy, $E = mN + \mathcal{E}$, includes the rest mass energy and is the appropriate approximation to equation (4). Here, $N \equiv \int \mathrm{d}^3x\, \boldsymbol{\Psi}^\dagger\boldsymbol{\Psi}$ is the conserved particle number resulting from the $\boldsymbol{\Psi} \to e^{i\alpha}\boldsymbol{\Psi}$ symmetry of nonrelativistic Lagrangian (7).

The equation of motion for $\boldsymbol{\Psi}$ is a nonlinear Schrödinger equation $i\partial_t\boldsymbol{\Psi} = -\nabla^2\boldsymbol{\Psi}/(2m) + \partial_{\boldsymbol{\Psi}^\dagger} V_{\rm nl}$.

Oscillon solutions.– The ground state solution of this nonlinear Schrödinger equation with a fixed particle number $N = N_\star$ can be obtained by extremizing $\mathcal{E} + \mu(N - N_\star)$ where μ is a Lagrange multiplier. Such a solution must have the form

$$\boldsymbol{\Psi}(t, \boldsymbol{x}) = \boldsymbol{\Psi}(\boldsymbol{x}) e^{i\mu t}, \tag{10}$$

where the profile $\boldsymbol{\Psi}$ satisfies

$$-\mu\boldsymbol{\Psi} = -\frac{1}{2m}\nabla^2\boldsymbol{\Psi} + \partial_{\boldsymbol{\Psi}^\dagger} V_{\rm nl}. \tag{11}$$

Note that in a Cartesian basis, $\boldsymbol{\Psi}(\boldsymbol{x}) = \sum_{j=1}^3 \psi_j(\boldsymbol{x}) e^{i\phi_j(\boldsymbol{x})}\hat{\boldsymbol{x}}_j$, and ψ_j and ϕ_j are real valued functions. The profile equation (11) contains a set of 6 equations for these 6 real functions.

We now hunt for the lowest energy, spatially localized solutions for a fixed particle number, keeping in mind that there might be multiple solutions that are local minima of the energy. We do not know *a priori* which one is the true ground state.

The spatial variation in the phases $\phi_j(\boldsymbol{x})$ costs gradient energy, so we will set these to be spatially independent. Thereafter, by shifting the time coordinate, we can always set one of these three phases (say ϕ_z) to zero. We are then left with the task of determining two phases $\phi_{x,y}$ and three spatially varying functions $\psi_{x,y,z}$.

Like the phase, the spatial variation of the direction of the vector field also costs gradient energy. As a result, we

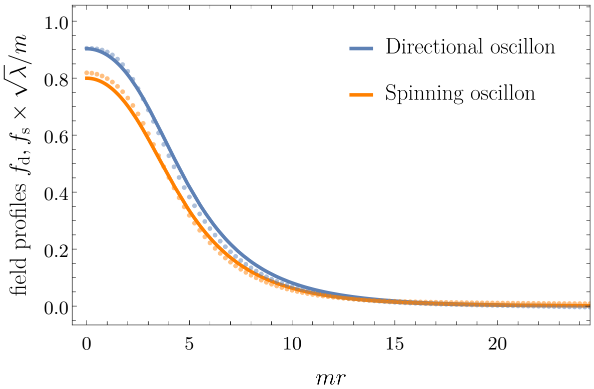

FIG. 2. Solid lines show the spatial profiles for directional and spinning oscillons derived using the nonrelativistic theory. Dots represent the appropriately averaged profiles extracted from simulations. For these profiles, we have $\omega = m - \mu \approx 0.975\,m$.

consider vector field configurations that point in the same direction at a given instant of time. We will restrict our attention to configurations with a spherically symmetric energy density. With these considerations, we focus on the following form of the field configuration:

$$\boldsymbol{\Psi}(\boldsymbol{x}) = \psi_x(r)e^{i\phi_x}\hat{\boldsymbol{x}} + \psi_y(r)e^{i\phi_y}\hat{\boldsymbol{y}} + \psi_z(r)\hat{\boldsymbol{z}}, \tag{12}$$

where $r = \sqrt{x^2+y^2+z^2}$.

Upon substituting equation (12) into equation (11), we get strong restrictions on the phases and profiles. Specifically, only two distinct classes of oscillons are allowed, which we refer to as directional and spinning oscillons respectively. These classes are represented by

$$\sqrt{\frac{2}{m}}\boldsymbol{\Psi}_{\rm d}(\boldsymbol{x}) = f_{\rm d}(r)\hat{\boldsymbol{z}}\,, \tag{13}$$
$$\sqrt{\frac{2}{m}}\boldsymbol{\Psi}_{\rm s}(\boldsymbol{x}) = f_{\rm s}(r)(\hat{\boldsymbol{x}} + i\hat{\boldsymbol{y}}), \tag{14}$$

where $f_{\rm d}$ and $f_{\rm s}$ satisfy the following profile equations

$$-\mu f_{\rm d} = -\frac{1}{2m}\nabla^2 f_{\rm d} - \frac{3\lambda}{8m}f_{\rm d}^3 + \frac{5\gamma}{16m}f_{\rm d}^5\,, \tag{15}$$
$$-\mu f_{\rm s} = -\frac{1}{2m}\nabla^2 f_{\rm s} - \frac{\lambda}{2m}f_{\rm s}^3 + \frac{\gamma}{2m}f_{\rm s}^5\,. \tag{16}$$

All other oscillons (with radially symmetric field components) in a given class are spatial rotations of these representative oscillons. The nodeless and spatially localized solutions can be obtained by a numerical shooting method and are shown in Fig. 2.

These two oscillons are also readily apparent if we decompose the field $\boldsymbol{\Psi}$ in an orthonormal polarization basis with respect to a fixed direction (see [51] for an explicit discussion). That is, $\boldsymbol{\Psi}(\boldsymbol{x}) = \sum_{m_s}\psi^{(m_s)}(\boldsymbol{x})\boldsymbol{\epsilon}_{\hat{z}}^{(m_s)}$, where $m_s = -1, 0, 1$ are the spin multiplicities, and $\boldsymbol{\epsilon}_{\hat{z}}^{(0)} = \hat{\boldsymbol{z}}, \boldsymbol{\epsilon}_{\hat{z}}^{(\pm1)} = (\hat{\boldsymbol{x}} \pm i\hat{\boldsymbol{y}})/\sqrt{2}$. Then, the directional and spinning oscillons are the ones with $\boldsymbol{\Psi}_{\rm d}(\boldsymbol{x}) \propto \boldsymbol{\epsilon}_{\hat{z}}^{(0)}$ and $\boldsymbol{\Psi}_{\rm s}(\boldsymbol{x}) \propto \boldsymbol{\epsilon}_{\hat{z}}^{(+1)}$, respectively [64].

While the spin density for the directional oscillon is zero, for the spinning oscillon it is given by $\boldsymbol{S}_{\rm s} = i\boldsymbol{\Psi}_{\rm s} \times \boldsymbol{\Psi}_{\rm s}^\dagger = mf_{\rm s}^2(r)\hat{\boldsymbol{z}}$. The total spin of the configurations are given by

$$\boldsymbol{S}_{\rm d}^{\rm tot} = 0\,, \quad \boldsymbol{S}_{\rm s}^{\rm tot} = N\hat{\boldsymbol{z}}\,, \tag{17}$$

where N is the particle number. Note that $N = \mathcal{O}[10^2]/\lambda$ can be macroscopically large for $\lambda \ll 1$ (see Fig. 3). The orbital angular momentum vanishes for both configurations.

In the nonrelativistic limit, the expressions for the real-valued vector field for directional and spinning oscillons are

$$\boldsymbol{W}_{\rm d}(t,\boldsymbol{x}) = f_{\rm d}(r)\cos(\omega t)\hat{\boldsymbol{z}}\,, \tag{18}$$
$$\boldsymbol{W}_{\rm s}(t,\boldsymbol{x}) = f_{\rm s}(r)\left[\cos(\omega t)\hat{\boldsymbol{x}} + \sin(\omega t)\hat{\boldsymbol{y}}\right]\,, \tag{19}$$

where $\omega = m - \mu$. In Supplemental Material B we also provide an "ϵ-expansion" scheme to obtain small-amplitude oscillons. Within this expansion, we provide subleading corrections which show deviations from spherical symmetry of the profiles as well as small corrections to the vector directions. However, this scheme (unlike the nonrelativistic expansion in this section) makes it difficult to obtain solutions in the stable regime.

Energy and Stability.– The particle number as well as the energy for these solutions as a function of $\omega = m - \mu$ are shown in Fig. 3. From the figures, it is clear that the directional and spinning solutions have different energy for fixed ω. Furthermore, for a fixed $N = N_{\rm d} = N_{\rm s}$, we have [65]

$$\mathcal{E}_{\rm d} < \mathcal{E}_{\rm s}\,. \tag{20}$$

In contrast, $\mathcal{E}_{\rm d} = \mathcal{E}_{\rm s}$ for vector solitons supported by gravitational interactions alone [51]. The reason for this degeneracy breaking in energy is the $\boldsymbol{S}\cdot\boldsymbol{S}$ term in $V_{\rm nl}$, which is absent in the gravitational case. It also prohibits construction of fractionally polarized solutions via linear superpositions of maximally polarized solitons [51].

As seen in Fig. 3, for each solution, there exist regimes where $dN/d\omega < 0$, as well as $\mathcal{E} < 0$ indicating classical and "quantum stability" respectively [66, 67]. Classical stability is the *less restrictive* of the two. Note that this assumes the number changing processes are suppressed as should be the case in the nonrelativistic regime. While suppressed, these processes are present in the relativistic theory and lead to a slow decay of the oscillons via relativistic radiation [68–74].

Relativistic Simulations.– Foregoing nonrelativistic approximations, we simulate vector oscillons on a 3 + 1-dimensional lattice by discretizing the relativistic equations (see Supplemental Material C for details). We confirm that the directional and spinning oscillons exist in

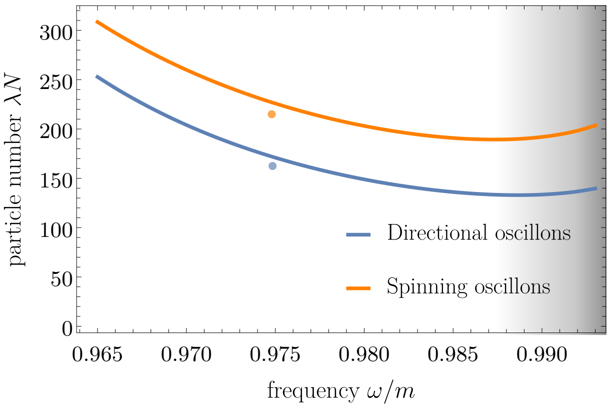

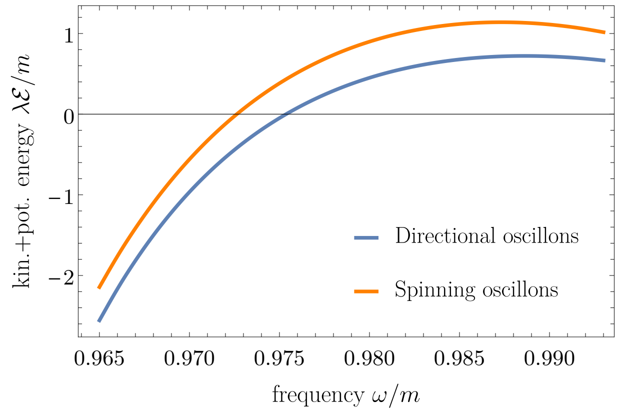

FIG. 3. Left panel: Total particle number N vs frequency $\omega = m - \mu$ for the two oscillons. The minimum of each curve determines the respective ω values below which the oscillons start to exhibit classical stability. The dots indicate the values obtained for oscillons from lattice simulations. Right panel: The sum of the kinetic and potential energy $\mathcal{E}$ as a function of ω. Negative $\mathcal{E}$ represents bound objects and hence "quantum stability" in the nonrelativistic limit.

the fully relativistic theory, and are long-lived compared to their oscillation period.

In order to see that the existence of vector oscillons is not too sensitive to the choice of initial conditions, we use a Gaussian ansatz $F(r) = Ce^{-r^2/R^2}$ with $C \lesssim m/\sqrt{\lambda}$ and $R \sim 10\, m^{-1}$ to initialize vector field components for our two different oscillons. Depending on the choice of C and R, the fields latch on to oscillon configurations with different dominant frequency ω (after an initial transient). For ease of comparison, we intentionally pick C and R so that in each case we get an oscillon with approximately the same $\omega \approx 0.975\, m$. This frequency is consistent with oscillons being classically stable according to the analysis in the previous section (see Fig. 2).

For the directional solitons, we start with an initial profile $\boldsymbol{W}(t, \boldsymbol{x})|_{t=0} = F(r)\hat{\boldsymbol{z}}$ and $\dot{\boldsymbol{W}}(t, \boldsymbol{x})|_{t=0} = 0$. Within $t = \mathcal{O}(10^2)\, m^{-1}$, this initial Gaussian profile settles into an oscillon configuration with frequency $\omega \approx 0.975\, m$ and the energy $E_{\rm d} \approx 164\, m/\lambda$. For this ω, the energy of the oscillon from the nonrelativistic approximation is $E_{\rm d} = mN + \mathcal{E} \approx 171 m/\lambda$ with a radius $R_{1/e} \approx 6 m^{-1}$ as seen in Figs. 3 and 2 respectively.

As the ansatz (18) is not fully compatible with the relativistic equations, a small deviation of the field configuration from the $\hat{\boldsymbol{z}}$ direction is expected, which is indeed observed in our simulations. See Supplemental Material C for snapshots of numerical profiles. In the quantities we have checked, such as profiles, energy etc., there is typically a few percent fractional difference between the results of the simulations and the nonrelativistic solutions. This difference is consistent with our expectation that relativistic corrections should be of order $|\nabla^2/m^2| \sim 1/(mR_{1/e})^2 = \mathcal{O}(10^{-2})$.

Taking advantage of a cylindrical symmetry exhibited by directinal oscillons, we carry out long-time simulations in effectively $2+1$ dimensions with absorbing boundary conditions. After an initial transient, the oscillon does not show significant energy loss for the duration of the simulations ($\sim 10^5 m^{-1}$). We note that the lifetimes may be longer because of non-trivial suppression in the decay rates as seen in the case of scalar oscillons [72, 73].

In order to obtain spinning oscillons, we start the simulation with $\boldsymbol{W}(t, \boldsymbol{x})|_{t=0} = F(r)\hat{\boldsymbol{x}}$, $\dot{\boldsymbol{W}}(t, \boldsymbol{x})|_{t=0} = F(r)\hat{\boldsymbol{y}}$. With these initial conditions, the field quickly settles into a spinning oscillon configuration with frequency $\omega \approx 0.975\, m$ and the energy $E_{\rm s} \approx 216\, m/\lambda$. Our analytic estimates yield $E_{\rm s} \approx 225\, m/\lambda$. Along with dominant components in the $x - y$ plane, we see small components in the $\hat{\boldsymbol{z}}$ direction. Moreover, the energy density deviates slightly from spherical symmetry. Once again, the analytic estimates from our nonrelativistic theory differ from the results from relativistic simulations by a few percent, consistent with our expectations.

Unlike the directional case, we cannot take advantage of symmetries to do a long-time simulation in effectively lower dimensions. However, we have verified that with absorbing boundary conditions, the spinning oscillon does not decay away for at least $\sim 10^3 m^{-1}$.

Discussions.– We have presented two new oscillon solutions in real-valued vector fields with attractive self-interactions. The oscillons are maximally polarized: the directional oscillon has zero intrinsic spin, while the spinning oscillon has maximum intrinsic spin equal to the occupation number of the oscillon in the nonrelativistic limit (i.e. $\boldsymbol{S}_{\rm tot} = \hbar N \hat{n}$). In the case of gravitational interactions alone, the two solitons (in the nonrelativistic limit) are degenerate in energy for fixed particle number, and can be appropriately superposed to form fractionally polarized solitons [51]. Here however, the presence of spin-spin interactions breaks this degeneracy, making the directional oscillon lower in energy, and furthermore prohibits fractionally polarized solitons.

We have confirmed that these oscillons are not too sensitive to the choice of initial conditions, and furthermore do not decay away for at least $10^3\, m^{-1}$ (see Supplementary Material D for further discussion of lifetimes as well as model parameters in two different production mechanisms for the vector field). A more detailed longer-timescale simulation, as well as analytic calculation of the decay rates (similar to [70–73]) are warranted. The lack of detailed sensitivity to initial conditions and their long lifetimes make them potentially relevant in astrophysical and cosmological scenarios.

The two oscillon solutions presented in this letter have approximately spherically symmetric energy density but not field configurations. However, there is another oscillon solution for which both the field and energy density are exactly spherically symmetric, known as the hedgehog oscillon [50, 75–79]. We find that this solution includes significant relativistic corrections towards its center, and is also higher in energy (and likely harder to form from generic initial conditions) than the two maximally polarized oscillons presented here. This will be the subject of future work.

The spin nature of the vector field, manifest in these oscillons, can lead to novel phenomenological implications. Collisions and mergers of dense vector oscillons can lead to gravitational wave production, which might be distinct from the scalar case [18–21, 23–25]. If the massive (dark) vector field kinetically mixes with the visible photon, namely $\mathcal{L} \supset (\sin\alpha/2)X^{\mu\nu}F_{\mu\nu}$ where $\sin\alpha$ is the mixing parameter and $F_{\mu\nu}$ is the field strength of the photon [80], collisions between polarized vector oscillons, or interaction with strong magnetic fields can also lead to specific outgoing radiation patterns based on oscillon polarization (see [27–29] for scalar case). If such vector oscillons exist today, and interact with terrestrial experiments [81–84], detectable signatures that depend on the polarization state of the vector field might be possible.

Formation mechanisms and production rates of vector oscillons, along with their early universe implications remain to be explored. The misalignment mechanism for production of dark photon dark matter [42, 44], where an oscillating inflaton or axion field transfers its energy to dark photons efficiently via a resonant instability, could produce vector oscillons resulting in additional small-scale structure in the early universe. Vector oscillons may also form naturally at the end of vector field inflation [85–87] analogous to scalar cases [9, 13], from "thermal" initial conditions [88], or by purely gravitational clustering in the early and contemporary universe [17, 89–91].

Beyond their cosmological context, we are currently exploring whether nonrelativisitic vector oscillons with isospin can be realized in multicomponent Bose-Einstein condensates with attractive self-interactions.

We would like to thank Ray Hagimoto, Siyang Ling, Andrew Long and Zong-Gang Mou (Rice University) for useful comments. HYZ would also like to thank Lingyuan Ji (Johns Hopkins University) for helpful discussions. This work is supported by a NASA ATP theory grant NASA-ATP Grant No. 80NSSC20K0518.

* hongyi@rice.edu
† mudit.jain@rice.edu
‡ mustafa.a.amin@rice.edu

[1] J. S. Russell, Report of the 14th Meeting of the British Association for the Advancement of Science, York, 1844.
[2] K. E. Strecker, G. B. Partridge, A. G. Truscott, and R. G. Hulet, Nature (London) **417**, 150 (2002), arXiv:cond-mat/0204532 [cond-mat.stat-mech].
[3] S. L. Cornish, S. T. Thompson, and C. E. Wieman, Phys. Rev. Lett. **96**, 170401 (2006), arXiv:cond-mat/0601664 [cond-mat.other].
[4] J. H. V. Nguyen, P. Dyke, D. Luo, B. A. Malomed, and R. G. Hulet, Nature Physics **10**, 918922 (2014).
[5] D. Luo, Y. Jin, J. Nguyen, B. Malomed, O. Marchukov, V. Yurovsky, V. Dunjko, M. Olshanii, and R. Hulet, Physical Review Letters **125**, 10.1103/physrevlett.125.183902 (2020).
[6] E. J. Copeland, M. Gleiser, and H.-R. Muller, Phys. Rev. D **52**, 1920 (1995), arXiv:hep-ph/9503217.
[7] A. Kusenko, Phys. Lett. B **406**, 26 (1997), arXiv:hep-ph/9705361.
[8] M. Gleiser and J. Thorarinson, Phys. Rev. **D79**, 025016 (2009), arXiv:0808.0514 [hep-th].
[9] M. A. Amin, R. Easther, H. Finkel, R. Flauger, and M. P. Hertzberg, Phys. Rev. Lett. **108**, 241302 (2012), arXiv:1106.3335 [astro-ph.CO].
[10] J. R. Bond, J. Braden, and L. Mersini-Houghton, JCAP **09**, 004, arXiv:1505.02162 [astro-ph.CO].
[11] M. A. Amin, P. Zukin, and E. Bertschinger, Phys. Rev. D **85**, 103510 (2012), arXiv:1108.1793 [astro-ph.CO].
[12] J. Ollé, O. Pujolàs, and F. Rompineve, JCAP **02**, 006, arXiv:1906.06352 [hep-ph].
[13] M. A. Amin and P. Mocz, Phys. Rev. D **100**, 063507 (2019), arXiv:1902.07261 [astro-ph.CO].
[14] A. Arvanitaki, S. Dimopoulos, M. Galanis, L. Lehner, J. O. Thompson, and K. Van Tilburg, Phys. Rev. D **101**, 083014 (2020), arXiv:1909.11665 [astro-ph.CO].
[15] J. C. Niemeyer and R. Easther, JCAP **07**, 030, arXiv:1911.01661 [astro-ph.CO].
[16] D. J. E. Marsh and A.-R. Pop, Mon. Not. Roy. Astron. Soc. **451**, 2479 (2015), arXiv:1502.03456 [astro-ph.CO].
[17] D. G. Levkov, A. G. Panin, and I. I. Tkachev, Phys. Rev. Lett. **121**, 151301 (2018), arXiv:1804.05857 [astro-ph.CO].
[18] S.-Y. Zhou, E. J. Copeland, R. Easther, H. Finkel, Z.-G. Mou, and P. M. Saffin, JHEP **10**, 026, arXiv:1304.6094 [astro-ph.CO].
[19] C. Palenzuela, P. Pani, M. Bezares, V. Cardoso, L. Lehner, and S. Liebling, Phys. Rev. D **96**, 104058 (2017), arXiv:1710.09432 [gr-qc].
[20] J. Liu, Z.-K. Guo, R.-G. Cai, and G. Shiu, Phys. Rev. Lett. **120**, 031301 (2018), arXiv:1707.09841 [astro-ph.CO].
[21] T. Helfer, E. A. Lim, M. A. G. Garcia, and M. A. Amin, Phys. Rev. D **99**, 044046 (2019), arXiv:1802.06733 [gr-qc].

[22] D. Croon, M. Gleiser, S. Mohapatra, and C. Sun, Phys. Lett. B **783**, 158 (2018), arXiv:1802.08259 [hep-ph].
[23] M. A. Amin, J. Braden, E. J. Copeland, J. T. Giblin, C. Solorio, Z. J. Weiner, and S.-Y. Zhou, Phys. Rev. D **98**, 024040 (2018), arXiv:1803.08047 [astro-ph.CO].
[24] T. Dietrich, F. Day, K. Clough, M. Coughlin, and J. Niemeyer, Mon. Not. Roy. Astron. Soc. **483**, 908 (2019), arXiv:1808.04746 [astro-ph.HE].
[25] K. D. Lozanov and M. A. Amin, Phys. Rev. **D99**, 123504 (2019), arXiv:1902.06736 [astro-ph.CO].
[26] T. Hiramatsu, E. I. Sfakianakis, and M. Yamaguchi, JHEP **03**, 021, arXiv:2011.12201 [hep-ph].
[27] M. P. Hertzberg, Y. Li, and E. D. Schiappacasse, JCAP **07**, 067, arXiv:2005.02405 [hep-ph].
[28] M. A. Amin and Z.-G. Mou, JCAP **02**, 024, arXiv:2009.11337 [astro-ph.CO].
[29] D. Levkov, A. Panin, and I. Tkachev, Phys. Rev. D **102**, 023501 (2020), arXiv:2004.05179 [astro-ph.CO].
[30] M. A. Amin, A. J. Long, Z.-G. Mou, and P. Saffin, JHEP **06**, 182, arXiv:2103.12082 [hep-ph].
[31] T. Helfer, D. J. E. Marsh, K. Clough, M. Fairbairn, E. A. Lim, and R. Becerril, JCAP **03**, 055, arXiv:1609.04724 [astro-ph.CO].
[32] E. Cotner, A. Kusenko, and V. Takhistov, Phys. Rev. D **98**, 083513 (2018), arXiv:1801.03321 [astro-ph.CO].
[33] F. Muia, M. Cicoli, K. Clough, F. Pedro, F. Quevedo, and G. P. Vacca, JCAP **07**, 044, arXiv:1906.09346 [gr-qc].
[34] J. Y. Widdicombe, T. Helfer, and E. A. Lim, JCAP **01**, 027, arXiv:1910.01950 [astro-ph.CO].
[35] Z. Nazari, M. Cicoli, K. Clough, and F. Muia, JCAP **05**, 027, arXiv:2010.05933 [gr-qc].
[36] K. Enqvist and J. McDonald, Phys. Lett. **B425**, 309 (1998), arXiv:hep-ph/9711514 [hep-ph].
[37] K. D. Lozanov and M. A. Amin, Phys. Rev. D **90**, 083528 (2014), arXiv:1408.1811 [hep-ph].
[38] T. Lee and Y. Pang, Phys. Rept. **221**, 251 (1992).
[39] S. L. Liebling and C. Palenzuela, Living Rev. Rel. **15**, 6 (2012), arXiv:1202.5809 [gr-qc].
[40] E. Y. Nugaev and A. V. Shkerin, J. Exp. Theor. Phys. **130**, 301 (2020), arXiv:1905.05146 [hep-th].
[41] P. W. Graham, J. Mardon, and S. Rajendran, Phys. Rev. D **93**, 103520 (2016), arXiv:1504.02102 [hep-ph].
[42] R. T. Co, A. Pierce, Z. Zhang, and Y. Zhao, Phys. Rev. D **99**, 075002 (2019), arXiv:1810.07196 [hep-ph].
[43] M. Bastero-Gil, J. Santiago, L. Ubaldi, and R. Vega-Morales, JCAP **04**, 015, arXiv:1810.07208 [hep-ph].
[44] P. Agrawal, N. Kitajima, M. Reece, T. Sekiguchi, and F. Takahashi, Phys. Lett. B **801**, 135136 (2020), arXiv:1810.07188 [hep-ph].
[45] E. W. Kolb, A. J. Long, and E. McDonough, Phys. Rev. D **104**, 075015 (2021), arXiv:2102.10113 [hep-th].
[46] E. W. Kolb, A. J. Long, and E. McDonough, Phys. Rev. Lett. **127**, 131603 (2021), arXiv:2103.10437 [hep-th].
[47] E. Babichev, L. Marzola, M. Raidal, A. Schmidt-May, F. Urban, H. Veermäe, and M. von Strauss, JCAP **09**, 016, arXiv:1607.03497 [hep-th].
[48] S. Alexander, L. Jenks, and E. McDonough, Phys. Lett. B **819**, 136436 (2021), arXiv:2010.15125 [hep-ph].
[49] P. A. Zyla *et al.* (Particle Data Group), PTEP **2020**, 083C01 (2020).
[50] P. Adshead and K. D. Lozanov, Phys. Rev. D **103**, 103501 (2021), arXiv:2101.07265 [gr-qc].
[51] M. Jain and M. A. Amin, Polarized solitons in higher-spin wave dark matter (2021), arXiv:2109.04892 [hep-th].
[52] M. Gleiser, N. Graham, and N. Stamatopoulos, Phys. Rev. D **82**, 043517 (2010), arXiv:1004.4658 [astro-ph.CO].
[53] Y. Sang and Q.-G. Huang, Oscillons during Dirac-Born-Infeld Preheating (2020), arXiv:2012.14697 [hep-th].
[54] L. E. Padilla, J. C. Hidalgo, and K. A. Malik, A new mechanism for primordial black hole formation during reheating (2021), arXiv:2110.14584 [astro-ph.CO].
[55] C. Menyuk, IEEE Journal of Quantum electronics **23**, 174 (1987).
[56] D. N. Christodoulides and R. Joseph, Optics letters **13**, 53 (1988).
[57] D. Rand, I. Glesk, C.-S. Brès, D. A. Nolan, X. Chen, J. Koh, J. W. Fleischer, K. Steiglitz, and P. R. Prucnal, Physical review letters **98**, 053902 (2007).
[58] Z.-Y. Sun, Y.-T. Gao, X. Yu, W.-J. Liu, and Y. Liu, Physical Review E **80**, 066608 (2009).
[59] F. Baronio, A. Degasperis, M. Conforti, and S. Wabnitz, Physical review letters **109**, 044102 (2012).
[60] For definiteness we set $\gamma = \lambda^2/m^2$, and we have verified that qualitative features of vector oscillons remain unchanged if this value is changed by $\mathcal{O}(\lambda^2/m^2)$. In the Supplemental Material A, we show that such an attractive potential indeed arises in the low-energy limit of a $U(1)$ Abelian-Higgs model with a heavy Higgs, in which $\gamma = (3/4)(\lambda^2/m^2)$.
[61] M. H. Namjoo, A. H. Guth, and D. I. Kaiser, Phys. Rev. D **98**, 016011 (2018), arXiv:1712.00445 [hep-ph].
[62] B. Salehian, M. H. Namjoo, and D. I. Kaiser, JHEP **07**, 059, arXiv:2005.05388 [astro-ph.CO].
[63] B. Salehian, H.-Y. Zhang, M. A. Amin, D. I. Kaiser, and M. H. Namjoo, JHEP **09**, 050, arXiv:2104.10128 [astro-ph.CO].
[64] In general for an arbitrary direction $\hat{n}$, the set $\{\boldsymbol{\epsilon}_{\hat{n}}^{(m_s)}\}$ is orthonormal in the sense that $\boldsymbol{\epsilon}_{\hat{n}}^{(m_s)\,\dagger} \cdot \boldsymbol{\epsilon}_{\hat{n}}^{(m_s')} = \delta_{m_s,m_s'}$, and $\sum_{m_s}\left[\boldsymbol{\epsilon}_{\hat{n}}^{(m_s)}\,\boldsymbol{\epsilon}_{\hat{n}}^{(m_s)\dagger}\right]_{ij} = \delta_{ij}$. Also note that the $m_s = -1$ state can be obtained by a rotation of the $m_s = 1$ state.
[65] For $\gamma = 0$, one can show analytically by appropriate scaling of the field and spacetime coordinates that $\mathcal{E}_\mathrm{d} = (4/9)\mathcal{E}_\mathrm{s}$ for $N_\mathrm{s} = N_\mathrm{d}$ with $\mathcal{E}_\mathrm{d}, \mathcal{E}_\mathrm{s} > 0$. Alternatively for fixed ω, $\mathcal{E}_\mathrm{d} = (2/3)\mathcal{E}_\mathrm{s}$, consistent with what we see at the right edge of the right panel in Fig. 3.
[66] R. Friedberg, T. Lee, and A. Sirlin, Phys. Rev. D **13**, 2739 (1976).
[67] D. Levkov, E. Nugaev, and A. Popescu, JHEP **12**, 131, arXiv:1711.05279 [hep-ph].
[68] G. Fodor, P. Forgacs, Z. Horvath, and M. Mezei, Phys. Rev. D **79**, 065002 (2009), arXiv:0812.1919 [hep-th].
[69] P. Grandclement, G. Fodor, and P. Forgacs, Phys. Rev. D **84**, 065037 (2011), arXiv:1107.2791 [gr-qc].
[70] K. Mukaida, M. Takimoto, and M. Yamada, JHEP **03**, 122, arXiv:1612.07750 [hep-ph].
[71] M. Ibe, M. Kawasaki, W. Nakano, and E. Sonomoto, JHEP **04**, 030, arXiv:1901.06130 [hep-ph].
[72] H.-Y. Zhang, M. A. Amin, E. J. Copeland, P. M. Saffin, and K. D. Lozanov, JCAP **07**, 055, arXiv:2004.01202 [hep-th].
[73] H.-Y. Zhang, JCAP **03**, 102, arXiv:2011.11720 [hep-th].
[74] D. Cyncynates and T. Giurgica-Tiron, Phys. Rev. D

103, 116011 (2021), arXiv:2104.02069 [hep-ph].
[75] A. Y. Loginov, Phys. Rev. D **91**, 105028 (2015).
[76] R. Brito, V. Cardoso, C. A. R. Herdeiro, and E. Radu, Phys. Lett. B **752**, 291 (2016), arXiv:1508.05395 [gr-qc].
[77] N. Sanchis-Gual, C. Herdeiro, E. Radu, J. C. Degollado, and J. A. Font, Phys. Rev. D **95**, 104028 (2017), arXiv:1702.04532 [gr-qc].
[78] N. Sanchis-Gual, F. Di Giovanni, M. Zilho, C. Herdeiro, P. Cerd-Durn, J. Font, and E. Radu, Phys. Rev. Lett. **123**, 221101 (2019), arXiv:1907.12565 [gr-qc].
[79] J. C. Bustillo, N. Sanchis-Gual, A. Torres-Forné, J. A. Font, A. Vajpeyi, R. Smith, C. Herdeiro, E. Radu, and S. H. W. Leong, Phys. Rev. Lett. **126**, 081101 (2021), arXiv:2009.05376 [gr-qc].
[80] A. Caputo, A. J. Millar, C. A. J. O'Hare, and E. Vitagliano, Dark photon limits: a cookbook (2021), arXiv:2105.04565 [hep-ph].
[81] A. Caldwell, G. Dvali, B. Majorovits, A. Millar, G. Raffelt, J. Redondo, O. Reimann, F. Simon, and F. Steffen (MADMAX Working Group), Phys. Rev. Lett. **118**, 091801 (2017), arXiv:1611.05865 [physics.ins-det].
[82] M. Baryakhtar, J. Huang, and R. Lasenby, Phys. Rev. D **98**, 035006 (2018), arXiv:1803.11455 [hep-ph].
[83] J. Chiles *et al.*, First Constraints on Dark Photon Dark Matter with Superconducting Nanowire Detectors in an Optical Haloscope (2021), arXiv:2110.01582 [hep-ex].
[84] Y. Chen, M. Jiang, J. Shu, X. Xue, and Y. Zeng, (2021), arXiv:2111.06732 [hep-ph].
[85] L. H. Ford, Phys. Rev. D **40**, 967 (1989).
[86] A. Golovnev, V. Mukhanov, and V. Vanchurin, JCAP **06**, 009, arXiv:0802.2068 [astro-ph].
[87] T. Koivisto and D. F. Mota, JCAP **08**, 021, arXiv:0805.4229 [astro-ph].
[88] E. Farhi, N. Graham, A. H. Guth, N. Iqbal, R. Rosales, and N. Stamatopoulos, Phys. Rev. D **77**, 085019 (2008), arXiv:0712.3034 [hep-th].
[89] H.-Y. Schive, T. Chiueh, and T. Broadhurst, Nature Phys. **10**, 496 (2014), arXiv:1406.6586 [astro-ph.GA].
[90] N. Blinov, M. J. Dolan, P. Draper, and J. Shelton, Phys. Rev. D **103**, 103514 (2021), arXiv:2102.05070 [astro-ph.CO].
[91] B. Eggemeier, B. Schwabe, J. C. Niemeyer, and R. Easther, Gravitational Collapse in the Post-Inflationary Universe (2021), arXiv:2110.15109 [astro-ph.CO].
[92] S. Weinberg, *The Quantum theory of fields. Vol. 1: Foundations* (Cambridge University Press, 2005).
[93] M. D. Schwartz, *Quantum Field Theory and the Standard Model* (Cambridge University Press, 2014).
[94] M. P. Hertzberg and M. Jain, Phys. Rev. D **99**, 065015 (2019), arXiv:1807.05233 [hep-th].
[95] L. Heisenberg, JCAP **05**, 015, arXiv:1402.7026 [hep-th].
[96] G. Fodor, P. Forgacs, Z. Horvath, and A. Lukacs, Phys. Rev. D **78**, 025003 (2008), arXiv:0802.3525 [hep-th].
[97] M. A. Amin and D. Shirokoff, Phys. Rev. **D81**, 085045 (2010), arXiv:1002.3380 [astro-ph.CO].
[98] M. A. Amin, Phys. Rev. **D87**, 123505 (2013), arXiv:1303.1102 [astro-ph.CO].
[99] M. Alcubierre, R. Becerril, S. F. Guzman, T. Matos, D. Nunez, and L. A. Urena-Lopez, Class. Quant. Grav. **20**, 2883 (2003), arXiv:gr-qc/0301105 [gr-qc].
[100] M. Alcubierre, *Introduction to 3+ 1 numerical relativity*, Vol. 140 (Oxford University Press, 2008).
[101] M. Gleiser and A. Sornborger, Phys. Rev. E **62**, 1368 (2000), arXiv:patt-sol/9909002.
[102] M. Alcubierre, G. Allen, B. Bruegmann, T. Dramlitsch, J. A. Font, P. Papadopoulos, E. Seidel, N. Stergioulas, W.-M. Suen, and R. Takahashi, Phys. Rev. **D62**, 044034 (2000), arXiv:gr-qc/0003071 [gr-qc].
[103] E. W. Kolb and A. J. Long, JHEP **03**, 283, arXiv:2009.03828 [astro-ph.CO].
[104] A. Ahmed, B. Grzadkowski, and A. Socha, JHEP **08**, 059, arXiv:2005.01766 [hep-ph].